Proceedings of 10th International Conference on Precision, Meso, Micro and Nano Engineering (COPEN 10)
December 07 – 09, 2017, Indian Institute of Technology Madras, Chennai – 600 036 INDIA

Effect of Process Parameters on Weld Bead Geometry and Element Segregation in Electron Beam Welding of INCONEL 718

Manu Thomas[a]*, Partha Saha[b], Girish Namboothiri[a], Radhakrishnan G[a], Snehil Srivastava[a]

[a]Vikram Sarabhai Space Centre, Trivandrum

[b]IIT Kharagpur, West Bengal, India

Abstract

INCONEL alloy 718 is a widely used super alloy in aerospace industry for applications involving high temperatures up to 650°C. Welding of INCONEL 718 is heavily depends on Electron Beam Welding (EBW) as key joining technique. Thus extensive characterization of EBW of Inconel 718 is required. In this present work, we study the effect of various process parameters viz. beam current, beam focus, welding speed etc. on the quality of welded coupons based on the observations from etched bead geometry. The larger underfill that found in sharp-focus samples compared to the up-focus samples is explained using Marangoni effect. At higher welding speeds uniform penetration and minimum underfill are observed. The extent of alloy element segregation due to changes in weld parameters and the effect of process parameters on weld bead geometry are investigated. We also discuss the reasons for changes in bead geometry and their implications.

Images from a Scanning Electron Microscope (SEM) reveal the presence of Nb rich phases in Austenitic matrix of weld bead. Formation of Nb rich phases in weld region is detrimental as it causes a drop in the percentage of Niobium (Nb) in bulk matrix. Nb segregation in root region was found to be less as compared to that of top region of the weld bead. Tensile strength of specimens were determined and these were in concurrence with the SEM observations on element segregation. Superior tensile strength values are observed for sharp focus cases as compared to up-focus cases. This behavior is further investigated by correlating changes in laves formation with the beam focus changes.

Keywords: Electron Beam Welding (EBW), Inconel Alloy 718, Heat Affected Zones (HAZ)

1. INTRODUCTION

Inconel 718 is a Ni–Cr–Fe-based super alloy. It is widely used in aerospace industry for applications that involves high temperatures up to 640°C. It can be easily fabricated, and possess good tensile, creep, fatigue, rupture strength. It is used in manufacture of fasteners and instrumentation parts. It has got good resistance to post weld cracking which is an important welding characteristic that increases its applicability.

Inconel alloy 718 shall be welded by Gas tungsten arc welding (GTAW), Laser beam welding (LBW) and Electron Beam Welding (EBW). Although the EB welding has some inherent advantages over other welding techniques on Inconel-718, the mechanical properties of EB welds are still considerably lower compared to the parent material (PM) properties. However, studies indicated that significant advantages in terms of mechanical properties can be achieved by controlling Laves phase formation and altering its morphology by employing beam oscillations techniques in EB welding. The mechanical properties of welded components are influenced by the microstructure of fusion zone (FZ), and heat-affected zone (HAZ).

Electron Beam Welding (EBW) is a fusion welding in which joint is made by heating the work piece due to impingement of the focused electron beam of very high kinetic energy on the work piece. When the electron beam hits the work piece, kinetic energy of the electron beam is getting converted into thermal energy, resulting in melting and even evaporation of the work material.

Janaki Ram et al. [1] observed that, the strength of Inconel 718 mainly depends on the gamma prime phase (γ'- phase) precipitation that occurs during heat treatment. Inconel 718 utilizes Niobium (Nb) as the prime strengthening element. The addition of Nb avoids the problem of strain age cracking and increases the weld strength. On the other hand, the separation of Nb in the inter dendrite areas, that occurs during the solidification process associated with the welding creates a severe constraint. This separation of Nb leads to the formation of an inter metallic phase called "Laves phase" represented as $(Ni, Fe, Cr)_2$ $(Nb, Ti, Mo, Si)_3$. The more the Nb separates out in the inter-dendrite regions, the larger is the volume of laves phase that is formed (Vincent, 1985) [2].

E.G.Vinayan et al [3] studied the effect of electron beam welding of solution treated Inconel 718 evaluating its tensile properties, fracture toughness, weld bead microstructure and micro hardness. Further to this, responses of the aforesaid parameters in EB weld specimens are compared with parent material properties.

GAO Peng et al. (2011) [4] observed that after solution and two-aging treatment of electron beam welded Inconel 718 super alloy thick plate, the γ-phase (Ni3Nb) precipitates in the grain boundary. Once the precipitation of δ-phase (equilibrium orthorhombic Ni3Nb precipitate) increases, γ' (Ni3(Al,Ti)) and γ" (Ni3Nb) will decrease because Nb is shared by all of them (Saied Azadian et al., 2004)[5]. The stress rupture and tensile properties of the weld are inferior compared to the coupons prepared with solution pre-treatment when aging heat treatment is done on weld coupons without post weld solution heat treatment, (Janakiram et al., 2004)[1].

Saied Azadian et al. (2004) observed that the maximum rate of δ phase precipitation happens at temperatures close to 900°C and have confirmed full dissolution of δ phase beyond the solvus temperature range. Improved mechanical properties are assured if the laves creation is controlled by a appropriate method during EB welding. As an example, a beam oscillation method can be used to decrease laves phase formation. Madhusudhana Reddy et al. (2009) [6] found that with appropriate beam oscillation, the laves morphology can be positively changed to get improved weld properties.

ISBN: 978-93-80689-28-9

J.K. Hong et al. [7] studied the microstructures and mechanical properties of Inconel 718 welds by CO_2 laser welding. They found that for Inconel 718 plate having 5mm thickness, minimum 6 kW of laser power was required to produce full penetration welds without defects such as porosities. This was taken as the base for setting the range of heat input required to get full penetration for our 6.6mm sample. The paper also mentions that the optimum focus position for maximum weld depth and defect-free weld was on the surface (sharp focus beam)

2. EXPERIMENTAL SETUP

The EBW machine used for welding the samples is EO Paton make KL134 model. The governing parameters of this particular machine are as follows:

- Chamber pressure: 2.6×10^{-4} torr
- Distance between EB gun and top surface of specimen: 245mm
- Focusing current:
    - sharp focus: 547mA, up focus by 2mm: 555mA & up focus by 4mm:563mA
- Power: 30 kW
- Accelerating voltage: 60 kV

Inconel alloy 718 plates of 6.5 mm thickness were selected for the study. 36 plates of size 75x 80x 6.5 mm were taken with suitable edge preparation and cleaning.

Fig 1. Samples after cutting to required dimensions

A theoretical heat input value was calculated based on the following assumptions:-

- Since thermal conductivity of Inconel 718 is very less (11.4 W/Km), heat loss due to conduction can be neglected.
- Since experiment was carried out in vacuum of the order 2 to 3 x 10-4torr, heat loss due to convection is not present.
- Heat loss due to radiation was also neglected.
- All material properties were assumed to remain same during welding.
- For welding to take place, temperature should be more than liquidus temperature and less than boiling temperature. Thus the weld pool was assumed to be at a mean temperature of this.

Thus it was assumed that all heat supplied was used to melt the material i.e. to form the weld pool.
The following equation was used:-

$$\frac{\eta P}{v} = A\rho(c_p \Delta T^* + L_f)$$

Where η = overall efficiency
P = power
v = welding speed
A = weld cross sectional area
ρ = density of material
C_p = specific heat capacity at constant pressure
ΔT^* = mean temperature of liquidus and boiling temperatures i.e. $(T_l + T_b)/2$
L_f = latent heat of fusion

The expected keyhole weld profile was plotted graphically with width of weld assumed as 4mm and with full penetration of 6.5mm.From this weld area calculated was 12.5 mm^2. Also overall efficiency was assumed as 0.9 considering the fact that heat loss associated with EBW of low conducting material like Inconel 718 is very minimum. Substituting these values in the above equation, theoretical heat input was found as

$$\frac{P}{v} = 121.76\ J/mm$$

We have Power, P = V*I
Where V = accelerating voltage = 60 kV &
I = beam current in mA

The experiment was carried out for 3 cases: -
Case 1. Sharp focus
Case 2. 2mm upfocus
Case 3. 4mm upfocus

For each case, 5 welding speeds were selected as 15mm/s, 20mm/s, 25mm/s, 30mm/s and 32mm/s and the corresponding beam currents were calculated.

Case 1: Sharp focus

At welding speed of 25mm/s and corresponding beam current of 50.733 mA, a trial run was carried out with bead on weld to validate these parameters. It was found that full penetration was not achieved with these parameters. Hence beam current was increased to 58 mA and subsequently to 62 mA, 66 mA and 70 mA with welding speed remaining the same. It was found that the best weld (good penetration and less underfill) was achieved with 66 mA beam current. In case of actual weld, beam current required is slightly higher than the case for bead on welds. Hence a beam current of 68 mA was selected for Case 1: Sharp focus at the welding speed of 25mm/s. Correspondingly actual heat input required also changed to 163.2 J/mm. Using this heat input, beam currents for other welding speeds were calculated (as in table 1) and welding was carried out.

Table 1 Welding Parameters for Case 1

	Set 1	Set 2	Set 3	Set 4	Set 5
Scan speed(mm/s)	15	20	25	30	35
Beam current(mA)	40.8	54.4	68	81.6	95.2

Case 2: 2mm upfocus

A bead on weld trial run was carried out at welding speed of 25mm/s and beam current same as that in case 1 i.e. 68 mA. The weld was found to be good (good penetration and fewer underfills). Hence the same parameters as used in Case 1 were used in this case also and good welds were obtained for every welding speed.
Case 3: 4mm upfocus

Again a bead on trial weld was carried out at welding speed of 25mm/s and beam current of 68 mA. However it was found that the weld was very poor. There was a drastic decrease in depth of penetration. Hence beam current was increased to 72 mA and subsequently to 76 mA, 80 mA, 84 mA, 88 mA, 92 mA, 96 mA and 100 mA with welding speed remaining same at 25 mm/s. It was found that the best weld (good penetration and less underfill) was achieved with 100 mA beam current. For actual welding, this was increase to 102 mA. Corresponding actual heat input required also changed to 244.8 J/mm. With this heat input value, beam currents for other welding speeds were calculated (as in table 2) and welding carried out.

Table 2 Welding Parameters for Case 3

	Set 1	Set 2	Set 3	Set 4	Set 5
Scan speed(mm/s)	15	20	25	30	35
Beam current(mA)	61.2	81.6	102	122.4	142.8

3. RESULTS AND DISCUSSIONS

3.1 Effect of Process Parameters on Weld Bead Geometry

The specimens after chemical etching were analyzed under a microscope to assess weld profile characteristics viz. width of weld, underfill, weld depth (as shown in Figure2) etc. This was done to understand the effect of various process parameters on weld bead geometry.

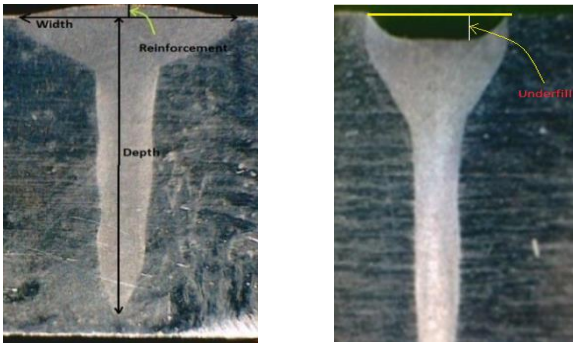

Figure 2 shows the weld profile attributes

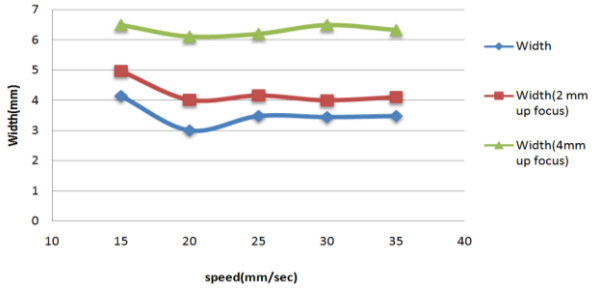

Figure 3 Bead width Vs speed graph for different focus

The bead width of weldment depends on the beam focus conditions. Samples prepared with up-focused beam have a broader reinforcement at the top compared to the samples done with a sharp-focused beam. Nevertheless, for a specific focus, the welding speed did not make a significant impact on weld bead width (Figure 3)

Reinforcement/under fill and root side penetration are plotted against speed as shown in figure 4.a & 4.b.With the welding parameters which give partial weld depth, reinforcement is observed in the bead geometry. From the Fig.4 a & b it can be observed that at 15 mm/s weld speed, reinforcement is present for both up focus cases (2mm and 4mm up focus) where the depth of weld is less than plate thickness. As the welding speed increased to 20mm/s we get non uniform penetration and high underfill in the bead geometry. But when the speed increases beyond 20mm/s, underfill is reduced and resulted in uniform penetration. Thus from these observations it is evident that at welding speed 30-35mm/s bead geometry is more uniform with less underfill. The similar trend was observed for sharp focus, 2mm up focus and for 4mm up focus.

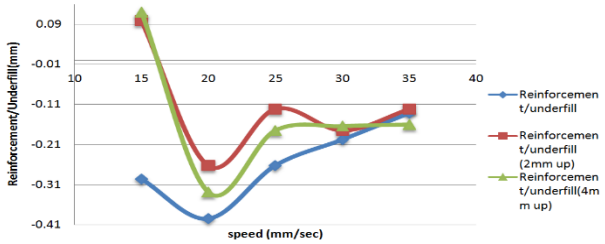

(a)

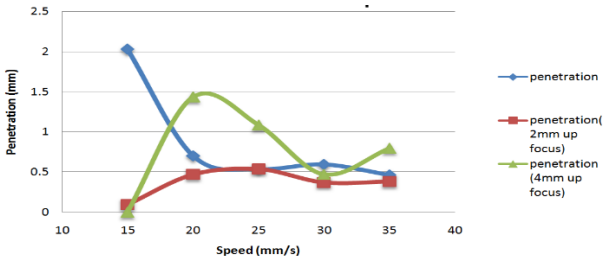

(b)

Figure 4 (a) Reinforcement/underfill Vs speed graph (b) Penetration Vs speed graph for different focuses.

For the electron beam heat source, a Gaussian power density distribution is approximated with the heat intensity being largest at the centre and falling towards the periphery [5]. As a result, a differential temperature exists in the molten weld pool with highest temperatures at the centre. This leads to the surface tension gradient within the weld pool. Molten metal at the weld centre that has the lowest surface tension is pulled in the direction of the regions with higher surface tension (Marangoni effect). This causes a depression in the molten weld pool and leads to the formation of weld underfill. In the case of sharp focused beam, a larger surface tension gradient exists inside the molten weld pool compared to the samples prepared by an up-focus beam. This explains the underfill profile that found in sharp-focus samples compared to up-focus samples (Figure 5a & 5b).

The area of cross section of weld bead is computed for all the samples and theoretical heat input was calculated. The cross-section area of the bead is increasing linearly with increase in beam current, thus theoretical heat input calculated based on bead area is also increasing. From figure 6a & 6b it can be seen that the theoretical heat input line is always at an offset from the actual heat input line. This may be due to the various heat losses due to conduction, vaporisation and the assumptions used while calculating theoretical heat input.

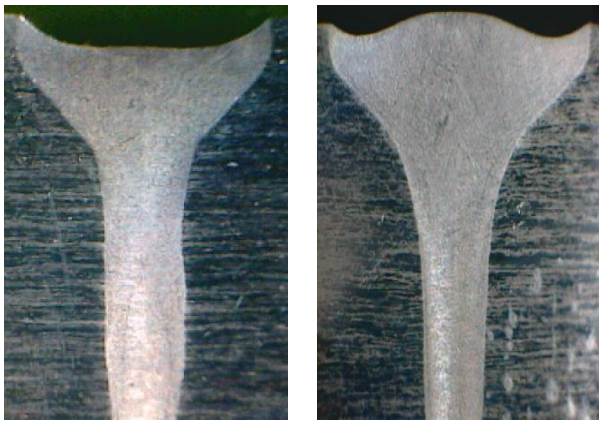

Figure 5(a): Underfill in sharp focus sample
Figure 5(b): Underfill in 4mm up focused sample

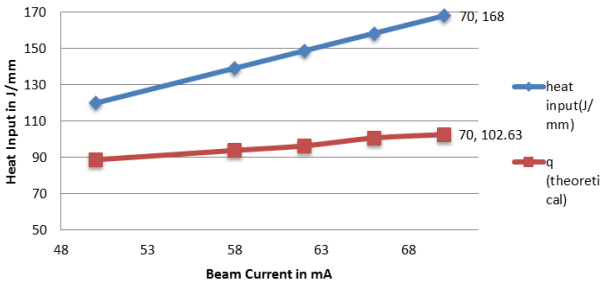

Figure 6 a Heat input Vs Beam current (sharp focus)

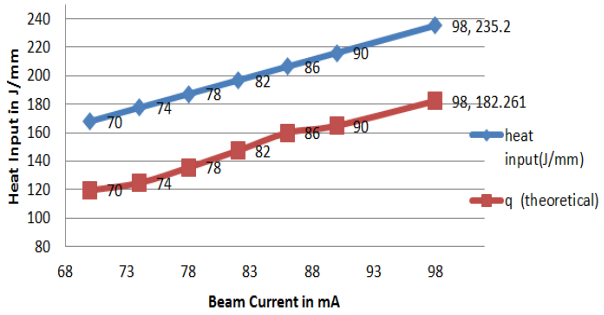

Figure 6 b Heat input Vs Beam current (4 mm up focus)

It is found that for sharp focus beam the difference between actual and theoretical heat input increases with beam current. This may be due to the increased vaporisation and other losses at higher beam current, since the heat intensity is also increases with beam current at sharp focus.

Figure 7 shows how theoretical heat input is related to the welding speed. It can be seen that as the welding speed increases, the theoretical heat input computed based on the cross-section area of the weld bead increases slightly. It may be due to the less conduction/evaporation losses at higher speeds compared to the lower speeds. The difference between the actual heat input and theoretical heat input attributes to all the heat losses including conduction losses, vaporization losses and the assumptions made during theoretical heat input calculation.

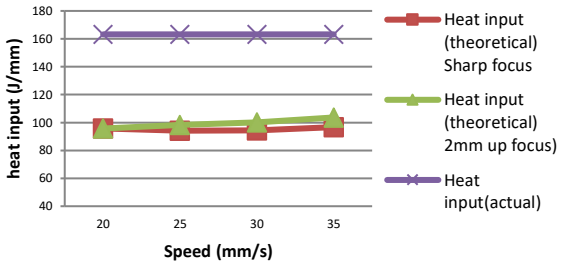

Figure 7 Heat input Vs speed graph

In the case of 4 mm up focused (figure 8), beam current/heat input required for full penetration was much more than that of sharp focus. This may be due to the reduced heat intensity at 4 mm up focus condition. In order to get full penetration through key hole formation some critical heat intensity is required below which depth of beam penetration falls drastically. At 4 mm up focus, heat intensity might have fallen below that critical value since the beam area at the surface is more than that of sharp focused beam. In order to increase the heat intensity at the joint, the beam current has to be increased, which results in an increased heat input to the weld bead.

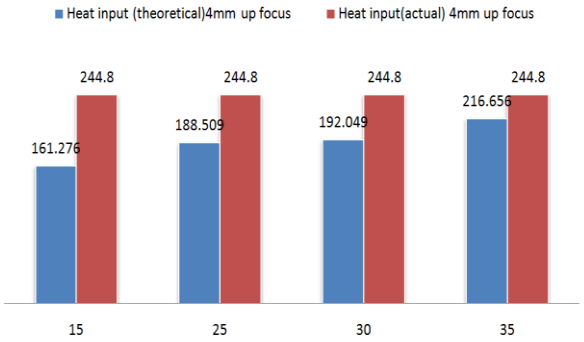

Figure 8 Heat input vs weld speed graph for 4mm up focus

3.2 Weld Pool Microstructure Observations Using SEM

In austenitic matrix of weld bead, the presence of Nb rich phases is revealed in SEM images (Figure 9). This phase contains significantly more Nb than the parent material. The formation of Nb rich phase in the weld region is harmful as it causes a reduction in the percentage of Nb in bulk weld matrix, which is a vital strengthening element in the matrix.

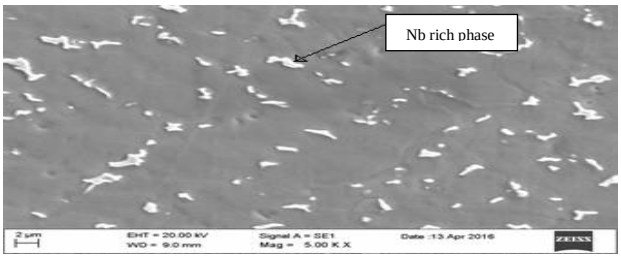

Fig 9: SEM image of weldment

Weight percentage of various alloy elements at the bulk matrix of the top and root portions of the weld samples are computed from an Energy Dispersive Spectroscopy (EDS) analysis. The observations are taken for both sharp and upfocus samples separately and the results are summarized in Table 3.

Due to the presence of Nb rich phases, Nb percentage in weld matrix (~3.6%) is small compared to the parent metal (~5.6%).

Table 3: Weight percentage of various element in top and bottom region

	Parent Metal	**Sharp Focus, 25mm/s,Top**	**Sharp Focus, 25mm/s,Root**	**4mm Up focus, 25mm/s,Top**	**4mm Up focus, 25mm/s,Root**
Element	Weight%	Weight%	Weight%	Weight%	Weight%
Ti K	1.12	0.78	0.98	1.05	0.83
Cr K	19.27	19.36	18.96	19.35	18.91
Fe K	18.77	20.51	19.96	20.13	19.46
Ni K	51.47	53.06	51.97	52.88	52.77
Nb L	5.66	3.14	3.61	2.73	4.31
Mo L	3.71	3.14	4.52	3.86	3.72

The percentage of Nb in Nb rich phase at top region of 4 mm up-focused samples is more compared to that of root region (21.86 % and 16.89 % respectively) (Figure 10 & 11). This leads to more Nb deficiency in the top region of samples welded with up-focused beam. At the root region Nb deficiency is less than the top region. Higher Nb content in Nb rich phases at the top portion of weld makes it more brittle and incapable of handling thermal stresses during welding [9].

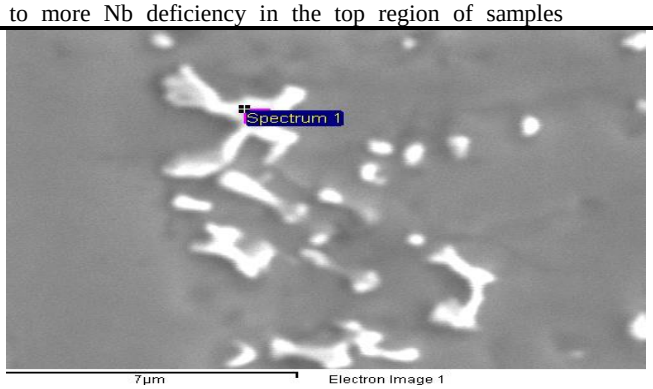

Element	Weight%
Ti K	2.07
Cr K	15.35
Fe K	13.64
Ni K	47.09
Nb L	21.86

Fig 10: Nb rich phases at top region

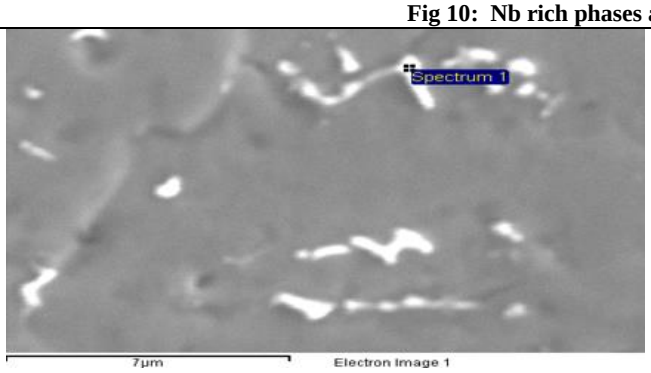

Element	Weight%
Ti K	1.32
Cr K	16.53
Fe K	14.81
Ni K	46.35
Nb L	16.89

Fig 11: Nb rich phases at root region

3.3 Tensile Testing Results

In this stud, a subsize specimen was used for tensile testing. Accordingly, specimen dimensions were set as per ASTM E8/E8M-13: "Standard Test Methods for Tension Testing of Metallic Materials" (2013). From each weld coupons, 3 tensile specimens were made and tensile strength of specimens were found out using universal testing machine. The results are as given in figure-12. For the given heat input, the difference in tensile strength of samples is found to be marginal.

For those specimens welded with a sharp focused beam, the tensile strength is marginally high (~892 MPa) compared to the up focused weld specimens (~872 Mpa). This variation in tensile strength can be due to the difference in Nb separation associated with laves phase formation which affects the weld

strength. In sharp focus samples Nb separation is less compared to samples welded with up focused beam.

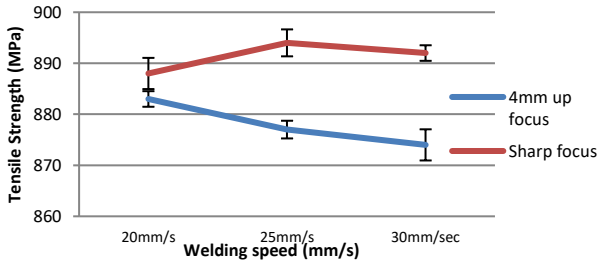

Fig 12: UTS Vs Welding Speed

4 CONCLUSION

The effect of process parameters in electron beam welding of Inconel 718 plates are investigated based on bead geometry observations. SEM/EDS analysis revealed the presence of Nb rich phases in Nb deficient matrix. More Nb segregation is observed at top portion of the weld bead compared to the root region. Tensile testing measurement is also taken and the results were confirmatory with the SEM/EDS findings. Following are the major conclusions made.

1) The underfill is observed in all the weld specimens welded at various process parameters. Nevertheless, the underfill is more in samples that are welded with sharp focused beam. This is described using Marangoni effect of temperature on surface tension of liquids.
2) The difference observed between actual heat input and theoretical heat input may be due to the various heat losses (conduction, radiation, vaporization) and the various assumptions made during the theoretical calculation.
3) Bead width remains the same for all beam current and welding speed combinations for a particular heat input and it increases with increase in heat input.
4) Reinforcement/underfill is affected by penetration. At high penetration, high underfill is observed and for insufficient penetration, reinforcement was observed.
5) The formation of Nb rich phases during the solidification of weld pool causes a drop in the percentage of Nb in the weld matrix compared to the parent metal. The Nb separation is more in the upper region of weld bead which is welded with up-focused beam compared to the weld samples welded at sharp focus.
6) The presence of brittle laves phases and higher Nb segregation from the bulk matrix leads to the tensile strength of up-focus samples being smaller than that of the sharp-focus samples.

References

[1] Janaki Ram, G.D., Venugopal Reddy, A., Prasad Rao, K., Madhusudhan Reddy, G., Microstructure and mechanical properties of Inconel 718 electron beam welds, Mater. Sci. Techno. 21, 1132–1138 (2005).

[2] Vincent, R., Precipltation around welds in the Nickel-base superalloy, inconel 718. H. H. Wills Physics Laboratory, University of Bristol (1985).

[3] E.G Vinayan,Mahesh Babu. B. R,Satheeshkumar A,Vinu Paul, R Sarath, Shibu Gopinath.,Electron Beam welding of Inconel 718,VSSC-MS 11-268.

[4] GAO Peng, ZHANG Kai-feng, ZHANG Bing-gang, JIANG Shao-song, ZHANG Bao-wei, Microstructures and high temperature mechanical properties of electron beam welded Inconel 718 superalloy thick plates, Trans. Non Ferrous Met.Soc. China 21, s315-s325 (2011).

[5] Saied Azadian, Liu-Ying Wei, Richard Warren., 2004. Delta phase precipitation in Inconel 718., Materials Characterization 53, 7– 16.

[6] Madhusudhana Reddy, G., Srinivasa Murthy., C.V., Srinivasa Rao, K., Prasad Rao, K., Improvement of mechanical properties of Inconel 718 electron beam welds-influence of welding techniques and postweld heat treatment. Int J Adv Manuf Technol 43:671–680 (2009).

[7] Hong, J.K., Park, J.H, Park, N.K., Eom, I.S., Kim, M.B., Kang, C.Y., Microstructures and mechanical properties of Inconel 718 welds by CO2 laser welding, Journal of materials processing technology. 201,515–520 (2008).

[8] Paolo Ferroa, Andrea Zambonb, Franco Bonolloa., Investigation of electron-beam welding in wrought Inconel706—experimental and numerical analysis., Materials Science and Engineering A 392, 94–105 (2005).

[9] Richard, N.L., Hung, X., Chaturvedi, M.C., Heat affected zone cracking in cast Inconel 718. Mater. Charact. 28, 179–187 (1992).

[10] Huanga, C.A., Wang, T.H., Lee, C.H., Han, W.C., a study of the heat-affected zone (HAZ) of an Inconel 718sheet welded with electron-beam welding (EBW). Materials Science and Engineering A 398, 275–281 (2005).

[11] Radhakrishna, C.H., Prasad Rao, K., Srivivas, S., Laves phase in superalloy 718 weld metals. J Mater Sci Lett 14:1810–1812 (1995).

[12] Thompson, R.G., Mayo, D.E., Radhakrishnam, B., Relationship between carbon content, microstructure and intergranular liquation cracking in cast nickel alloy 718. Metall. Trans. A 22, 557–567 (1991).

[13] Vishwakarma, K.R., Richards, N.L., Chaturvedi, M.C., HAZ microfissuring in EB welded ALLVAC 718 plus alloy. In: Procedings of Superalloy 718, 625 and Derivatives, pp. 637–647 (2005).

[14] Girish.N.Namboodiri., Manu Thomas., Abhinand Karna., Snehil Srivastava., Paul G Panicker., Shibu Gopinath., quality assessment of electron beam welds of inconel-718 plates using phased array ultrasonics and its comparison with radiography inspection (2015)